Available online at www.sciencedirect.com
SCIENCE DIRECT®
Journal of Nuclear Materials 329–333 (2004) 507–512
journal of nuclear materials
www.elsevier.com/locate/jnucmat

Effects of irradiation and post-irradiation annealing on the thermal conductivity/diffusivity of monolithic SiC and f-SiC/SiC composites

G.E. Youngblood *, D.J. Senor, R.H. Jones

Materials Science Division, P8-15, Pacific Northwest National Laboratory, 902 Battelle Blvd., P.O. Box 999, Richland, WA 99352, USA

Abstract

Laser flash thermal diffusivity measurements were made on high-purity monolithic CVD-SiC and 2D f-SiC(Hi-Nicalon^{TM})/ICVI-SiC composite samples before and after irradiation (250–800 °C, 4–8 dpa-SiC) and after post-irradiation annealing composite samples to 1200 °C. For irradiated CVD-SiC, the defect concentrations at saturation were estimated to range from 25 300 appm (250 °C) down to 940 appm (800 °C). The transverse thermal conductivity ratios after-to-before irradiation (K_{ir}/K_o) determined at the irradiation temperatures ranged from: 0.044 (250 °C) up to 0.12 (800 °C) for irradiated CVD-SiC and 0.18 (330 °C) up to 0.29 (800 °C) for the irradiated Hi-Nicalon^{TM} composite. Analysis of thermal diffusivity values for the Hi-Nicalon composite measured in air, argon, helium and vacuum indicated that thermal conductivity degradation occurred primarily due to point defect accumulation in the matrix component. After annealing to 1200 °C and cooling to ambient, fiber/matrix debonding occurred due to net shrinkage in the fiber and PyC interface components.

1. Introduction

Silicon carbide (SiC) exhibits excellent dimensional and thermodynamic stability, low activation and after heat, high strength and stiffness, relatively high thermal conductivity, and low electrical conductivity. For these reasons, SiC is considered a candidate structural material for fusion power reactor (FPR) first wall and blanket applications. Because SiC is a brittle ceramic material, continuous fiber-reinforced SiC composites (f-SiC/SiC), which exhibit toughness and psuedo-plastic behavior, are of more interest for certain FPR designs [1]. One of the major issues concerning the use of f-SiC/SiC for FPR applications is the rather large degradation of its thermal conductivity during neutron irradiation [2].

Thermal conductivity in SiC is controlled by phonon transport, which is sharply reduced when point defects are introduced. For irradiation temperatures below ~800 °C, where only free interstitials are mobile, the accumulation of point defects saturates [3]. As the irradiation temperature increases, recombination is more likely than stable interstitial clustering and the quasi-equilibrium concentration of defects decreases. Thus, for saturation conditions the relative reduction in the SiC thermal conductivity decreases in a manner similar to its swelling reduction with increasing irradiation temperature. Examination of SiC swelling data at various irradiation temperatures and doses suggests that saturation occurs for ~2 dpa-SiC at 200 °C and decreases continuously to ~0.4 dpa-SiC at 800 °C [4]. If the irradiated SiC is heated to temperatures above the irradiation temperature, the radiation-induced defects anneal out and the thermal conductivity recovers, also in a manner similar to swelling recovery in irradiated and annealed SiC [3].

In this report, the fundamental aspects of thermal conduction for irradiated ultra high-purity, monolithic

* Corresponding author.
E-mail address: ge.youngblood@pnl.gov (G.E. Youngblood).

0022-3115/$ - see front matter © 2004 Elsevier B.V. All rights reserved.
doi:10.1016/j.jnucmat.2004.04.111

chemical vapor deposited SiC (CVD-SiC) are examined. A strategy based on the analysis of the reciprocal thermal diffusivity temperature dependence is used to estimate point defect concentrations at saturation for neutron irradiated CVD-SiC at various temperatures. Then the thermal diffusivity degradation for a Hi-Nicalon^{TM} f-SiC/SiC composite after oxidation, irradiation and post-irradiation annealing treatments is assessed.

2. Experimental

2.1. Materials

A CVD-SiC (impurity concentrations <5 wppm) made by Morton Advanced Materials (now Rohm and Haas) was examined [5]. In the CVD process, methyltrichlorosilane gas is decomposed at ~1350 °C onto a carbon substrate at a growth rate of ~0.1 mm/h. The crystal structure is fcc (3C polytype β-SiC). The grain size is between 5 and 10 μm in the plane parallel to the substrate, but the grains are elongated in the ⟨1 1 1⟩ growth direction perpendicular to the substrate. There is no porosity in CVD-SiC (theoretical density 3.21 g/cm^3), but atomic layer stacking faults on the {1 1 1} planes are common. Because impurities are few in CVD-SiC, phonon scattering is primarily due to the faulted structure at low temperature as suggested by the close match between the calculated phonon mean free path and the characteristic spacing of the faults observed by TEM (20–50 nm) [6]. The thermal conductivity is slightly anisotropic because of the grain growth texture with the in-plane thermal conductivity being about 20% higher than in the growth direction. However, other properties (i.e., elastic modulus, strength and thermal expansion) are considered isotropic [5].

The f-SiC/SiC composite examined was made with plain weave Hi-Nicalon^{TM} fabric in a 0–90° layup by DuPont using the isothermal CVI-process with either a 'thin' (0.11 μm) or a 'thick' (1.04 μm) pyrolytic carbon (PyC) fiber coating applied by CVD prior to matrix infiltration. Four thermal diffusivity samples of each type (9.3 mm dia. × 2.3 mm thick) were diamond-cored from plates with their as-deposited flat surfaces retained. The bulk density values, determined by simple weighing and measuring of the disc dimensions, were in the range 2.50–2.60 g/cm^3. Cross-sectional SEM views of polished surfaces revealed a typical multi-layer fabric/matrix macroscopic structure for this 2D f-SiC/SiC composite [7].

2.2. Irradiation and test conditions

The thermal diffusivity (α) for the unirradiated and irradiated CVD-SiC and f-SiC/SiC discs was measured in air from RT to ~400 °C by the laser flash method described elsewhere [8]. The effective transverse thermal conductivity (K_{eff}) was determined from the product of measured α and bulk density values and the calculated specific heat capacity values. After pre-irradiation α-measurements were made, the same discs were sealed in helium-filled capsules. Different samples were irradiated at constant, but different temperatures (252–800 °C) in the HFIR reactor at ORNL to doses of 5–8 dpa-SiC, i.e., well above saturation for SiC.

After irradiation, a separate 'high' temperature laser flash system (contained inside a steel bell jar so that α-measurements could be made in vacuum, argon or helium) was used from 200 °C up to 1200 °C. In addition, the f-SiC/SiC samples were annealed in situ in this system to 1200 °C in argon. The PyC fiber coating was removed from other unirradiated f-SiC/SiC samples (two with each fiber coating thickness) by heating in air for 15 h at 700 °C. The coating 'burn-out' temperature was about 100 °C below that where significant SiO_2 formation begins, so the f/m interfaces were not sealed off.

3. Results and discussion

3.1. CVD-SiC

In Fig. 1, $\alpha(T)$-data for CVD-SiC samples irradiated at different temperatures are graphically presented as $1/\alpha$ vs temperature (K). The solid line represents the average unirradiated $1/\alpha$-values for the eight samples.

The individual $\alpha(T)$-curves for the unirradiated CVD-SiC samples exhibited characteristic $\sim 1/T$ temperature dependence, but also a significant spread (±20%). Importantly, repeated measurements on the same sample typically reproduced α-values to ±5%. Sample-to-sample variations were likely caused by subtle differences in microstructure even though the discs were cut from the same plate. The ±20% spread in the $\alpha(T)$-curves illustrates the importance of monitoring changes in diffusivity due to radiation effects for the same sample before and after irradiation.

The $1/\alpha$-data exhibit linear dependence with increasing temperature. Linear least squares fits to the data, $1/\alpha = A + B(T)$, are shown as dashed lines in Fig. 1. The A- and B-values determined from the fits are listed in Table 1 along with the sample irradiation conditions. Also, the defect mean free paths (λ_d) and the point defect concentrations (X), estimated by a method described by Senor [8], are listed in Table 1.

The linear fits of the $1/\alpha$-data over the RT-400 °C range are exceptionally good with correlation coefficients R^2 near 0.99. The calculated λ_d-values decrease continuously from ~22 nm (~50 lattice constants) for unirradiated CVD-SiC down to 0.74 nm (~2 lattice constants) for the sample irradiated at the lowest tem-

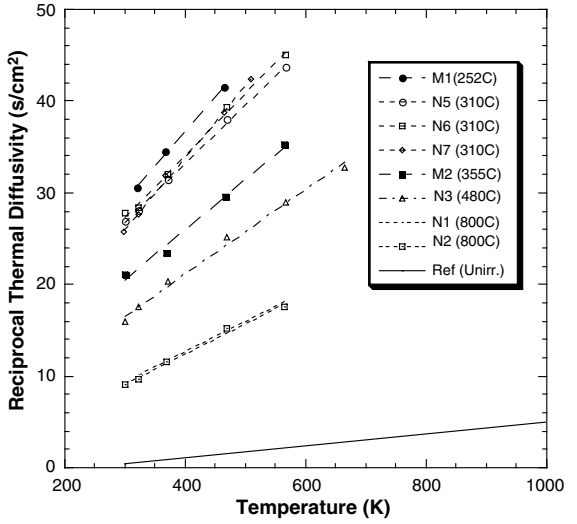

Fig. 1. Comparison of the reciprocal thermal diffusivity values determined for eight irradiated Morton™ CVD-SiC samples (irradiation temperature shown in parenthesis) with the average pre-irradiation values (solid line).

perature (252 °C). The calculated defect concentration for unirradiated CVD-SiC is less than 1 appm, which is consistent with the manufacturer's value of <5 wppm impurities. The defect concentrations for the irradiated CVD-SiC samples decrease continuously from ~25 000 to 940 appm as the irradiation temperature increases from 252 to 800 °C. The small concentration of intrinsic defects in comparison to the extrinsic irradiation defect concentrations illustrates why CVD-SiC makes an ideal irradiation damage monitor.

For engineering applications, the ratio of the irradiated-to-unirradiated thermal conductivity values (K_{ir}/K_o) evaluated at the irradiation temperature is a useful quantity because K_{ir} is the steady-state value expected during irradiation at saturation. Because the neutron irradiation will have only a relatively small effect on the bulk density and heat capacity, $K_{ir}/K_o \approx \alpha_{ir}/\alpha_o$. The estimated K_{ir}/K_o-ratio for each irradiated sample is listed in Table 1, and the temperature dependence of K_{ir}/K_o is graphically presented in Fig. 2. Similar K_{ir}/K_o-data reported by Rohde [9] and by Senor [6] for CVD-SiC, and reported by Thorne [10] for high-purity but somewhat porous β-SiC also are plotted.

In Fig. 2, the general trend that the K_{ir}/K_o-ratio increases as the irradiation temperature increases reflects the relative dominance of temperature independent point defect phonon scattering in the lower temperature range, while the temperature dependent phonon–phonon scattering becomes relatively more important with increasing temperature. The curve for high purity CVD-SiC represents a lower limit for SiC-based materials with $K_{ir}/K_o \sim 0.05$ at 200 °C and only gradually increasing up to ~0.12 by 800 °C. For irradiation temperatures above 800 °C, an apparent transition occurs where the K_{ir}/K_o-curve turns upward with an increasing slope until at 1100 °C the ratio is ~0.6. Above ~800 °C, the defect structure formed by the highly mobile irradiation-induced Si- and C-interstitials must become relatively coherent with the surrounding SiC matrix and presents less effective phonon scattering centers. Furthermore, the saturation condition appears to occur for equivalent doses larger than ~1 dpa-SiC as evidenced by the dose dependence observed at 1100 °C.

3.2. f-SiC/SiC

In Fig. 3, the measured $\alpha(T)$-values for the Hi-Nicalon™ f-SiC/SiC composites with a 'thick' PyC interface are presented for various conditions. The conditions were: [1] average $\alpha(T)$-values for four as-received samples (heavy solid line) and [2] average $\alpha(T)$-values for two unirradiated samples with PyC interface removed by oxidation (light solid line). Then for two irradiated samples D1 and D2 (both irradiated at 355 ± 35 °C to 7.1 dpa-SiC) in sequence of performance: [3] $\alpha(T)$-values in air (dashed lines), [4] $\alpha(T)$-values in vacuum (short

Table 1
Irradiation conditions and defect mean free path, point defect concentration and K_{ir}/K_o estimates for CVD-SiC samples

Sample ID	Irradiation temperature (°C)	Dose (dpa-SiC)	A (s/cm²)	B (s/cm² K)	R^2	λ_d (nm)	X (appm)	K_{ir}/K_o ($\approx \alpha_{ir}/\alpha_o$)
M1	252 ± 19	7.9	6.497	0.0755	0.9993	0.74	25 300	0.044
N5	310 ± 20	5.0	7.624	0.0641	0.9986	0.81	19 200	0.050
N6	310 ± 20	5.1	7.257	0.0671	0.9957	0.80	20 500	0.047
N7	310 ± 20	5.2	2.743	0.0778	0.9984	0.81	19 300	0.046
M2	355 ± 33	7.1	4.016	0.0548	0.9948	1.05	8900	0.067
N3	480 ± 20	6.1	2.827	0.0460	0.9931	1.29	4800	0.062
N1	800 ± 10	6.8	−0.628	0.0332	0.9893	2.21	960	0.134
N2	800 ± 10	6.9	−0.745	0.0330	0.9937	2.25	920	0.113
Ref.	–	–	−0.824	0.0054	0.9986	22.2	0.9	–

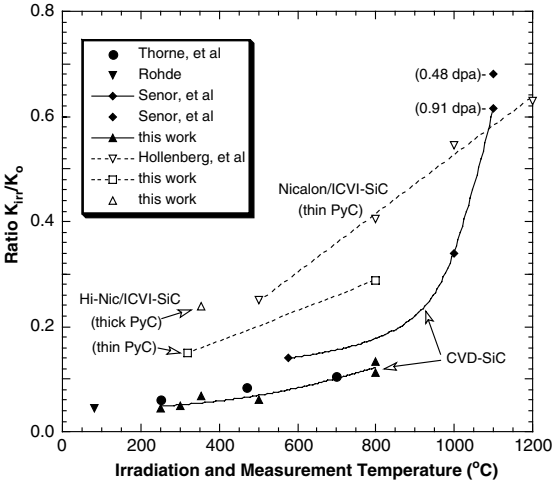

Fig. 2. Ratio K_{ir}/K_o, measured at the irradiation temperature for high-purity CVD-SiC and for two types of 2D f-SiC/SiC.

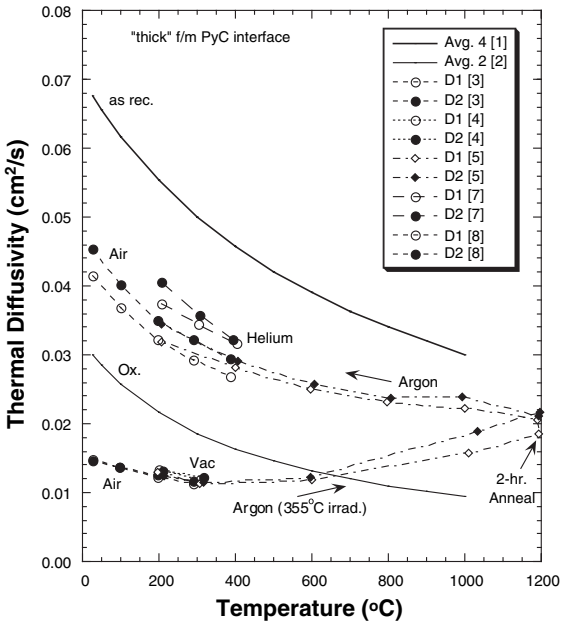

Fig. 3. Thermal diffusivity of 2D Hi-Nicalon™/ICVI-SiC composites with a 'thick' PyC interface for various unirradiated and irradiated conditions. See text for key.

dashed lines), [5] $\alpha(T)$-values in argon during in situ annealing from about 200 °C up to 1200 °C (2-h hold time) and after as the temperature was decreased back to 200 °C (dash-dot lines), [7] $\alpha(T)$-values in helium from 200 to 400 °C (long dashed lines), and finally [8] $\alpha(T)$-values in air again from RT up to 400 °C (dashed lines).

When the PyC interfaces were removed by oxidation, the α-values dramatically decreased to about 40% of their as-received values. Thermal decoupling of only the individual fiber filaments cannot account for this dramatic decrease. In fact, 85% of the fiber bundles in their entirety (i.e., including the matrix material contained within the bundles) must be thermally decoupled from the remaining matrix for thermal conductivity model predictions to predict observed results. The $\alpha(T)$-values of the oxidized samples also were measured in vacuum and in helium atmospheres. Compared to the values measured in air, the α-values increased by 15–30% when measured in helium, and decreased by 20–40% when measured in vacuum (data not shown in Fig. 3). Such effects are expected for composites with physical gaps formed at numerous f/m interfaces where the interfacial conductance depends upon the thermal conduction of the atmosphere within these gaps [7].

When the $\alpha(T)$-measurements were made in vacuum or argon after irradiation, close agreement with $\alpha(T)$-values measured in air was observed in the 200–350 °C overlap region. Apparently, at this point physical f/m gaps did not exist in the irradiated composites even though the matrix was expected to swell ~0.8% and the Hi-Nicalon™ fiber was expected to shrink ~1.7%. The radial swelling in the irradiated PyC fiber coating with its textured microstructure is expected to be >2% (with a commensurate axial shrinkage of ~0.7%). At least it is plausible that the expected swelling in the 'thick' PyC interface compensated somewhat for the differential shrinkage-swelling between the fiber and matrix components for the particular irradiation temperature and dose conditions, and significant f/m thermal decoupling did not occur.

Once the annealing temperature exceeded the irradiation temperature, the $\alpha(T)$-values increased with further increase in temperature in three steps up to 1200 °C, where the samples were held for two h to anneal the irradiation induced defects. After the 2-h anneal, the $\alpha(T)$-values at 1200 °C recovered to about 70–80% of their unirradiated values. Further $\alpha(T)$-measurements were made in argon as the temperature was then decreased in several steps from 1200 °C down to 200 °C. The argon atmosphere was replaced with helium and $\alpha(T)$-measurements were repeated over the 200–400 °C range. The samples were remounted in the air system and $\alpha(T)$-measurements were made from RT to 400 °C. The $\alpha(T)$-values measurements made in air or argon atmospheres agreed in the overlap temperature range, but were ~20% greater when measured in the helium atmosphere.

Apparently, the relative shrinkage-swelling situation changed when the irradiated and annealed composites were cooled after annealing. Expected shrinkage in the irradiated Hi-Nicalon™ fiber, caused by irreversible recrystalization and grain growth, should be permanent. In contrast, the swelling in the irradiated SiC matrix caused by accumulation of point defects should be

reversible when the defects recombine during annealing. The final situation should be a matrix with dimensions similar to the pre-irradiation conditions, while the fiber dimensions should be significantly reduced. Although the shrinkage-swelling situation in the irradiated and annealed PyC interface is more complex, significant physical f/m separation must have occurred in the irradiated, annealed and cooled composites. A thermal conductivity model based on the individual constituent conductivity contributions was used to predict expected α-values from RT to 200 °C for the Hi-Nicalon™ composite assuming complete thermal decoupling of the fiber constituent, but with no other changes in the matrix or in the porosity factors. The predicted $\alpha(T)$-values closely matched the observed magnitudes and slopes of the $\alpha(T)$-values measured after annealing, which suggests that the major contribution to K_{eff} for the irradiated and annealed Hi-Nicalon™ f-SiC/SiC with a 'thick' interface was conductivity in the continuously interconnected matrix, far different from the case with the PyC interface removed by oxidation where entire bundles became decoupled.

When the Hi-Nicalon™ composite with a 'thin' PyC interface was irradiated at 330 or at 800 °C and then taken through the same measurement and annealing sequence, the $\alpha(T)$-values were different in different atmospheres just after irradiation (data not shown). Apparently radial swelling in the irradiated 'thin' PYC interface was insufficient to close the f/m gap and at least partial thermal decoupling of the fibers from the matrix occurred during the irradiation.

After irradiation to doses above saturation but before annealing, the Hi-Nicalon™ fibers in the composite likely densified and shrunk while the matrix swelled. At this point, the expected f/m gap would be approximately the same for the composites with either the 'thin' or the 'thick' PyC interface. However, the net radial swelling of the 'thick' coating is ≈X10 that of the 'thin' coating (if the two PyC coatings behave similarly during irradiation), hence is more likely to close the gap. A rough estimate suggests that this should occur for a dose between 2–10 dpa-SiC for the 'thick' coating case. In contrast, the gap closure would not occur until doses exceeded ≈20 dpa-SiC for the 'thin' coating case.

The K_{eff}-values calculated from the $\alpha(T)$-data ranged from a maximum 15 W/m K at 200 °C down to 8–10 W/m K at 1000 °C for both Hi-Nicalon™ f-SiC/SiC composites [7]. The estimated $K_{\text{ir}}/K_{\text{o}}$-values also are shown in Fig. 2 along with similar data for a 2D f-SiC/SiC composite made with first generation Nicalon™ CG fabric [11]. In f-SiC/SiC composites, K_{eff} is greatly influenced by porosity and other structural features, and the addition of irradiation point defects has a relatively smaller effect on the conductivity degradation. Thus, the curve through the Hi-Nicalon™ composite data as well as the Nicalon™ CG data roughly marks an upper limit for the $K_{\text{ir}}/K_{\text{o}}$-ratio for SiC-based materials as compared to the lower limit curve for the CVD-SiC material. Interestingly, the $K_{\text{ir}}/K_{\text{o}}$-ratio for the Hi-Nicalon™ composite with a 'thick' PyC interface lies considerably above the line between the ratios for the Hi-Nicalon™ composite with a 'thin' PyC interface, again suggesting that f/m thermal decoupling had not occurred for the 'thick' PyC interface composite.

4. Summary

For irradiated CVD-SiC, the defect concentrations at saturation were estimated to range from 25 300 appm (250 °C) down to 940 appm (800 °C). The transverse thermal conductivity ratios after-to-before irradiation ($K_{\text{ir}}/K_{\text{o}}$) determined at the irradiation temperatures ranged from: 0.044 (250 °C) up to 0.12 (800 °C) for irradiated CVD-SiC and roughly 0.18 (330 °C) up to 0.29 (800 °C) for the irradiated Hi-Nicalon™ composites. Analysis of thermal diffusivity values for the Hi-Nicalon™ composite measured in air, argon, helium and vacuum indicated that thermal conductivity degradation occurred primarily due to irradiation-induced point defect accumulation in the matrix component. After annealing to 1200 °C and cooling to ambient, f/m debonding occurred due to net permanent shrinkage in the fiber and PyC interface components.

Acknowledgements

The irradiation tests were performed as part of the US/Japan JUPITER fusion materials collaboration. The Pacific Northwest National Laboratory is operated by Battelle Memorial Institute for the US Department of Energy under contract DE-AC 06-76RLO 1830.

References

[1] A.R. Raffrey, R. Jones, G. Aiello, M. Billone, L. Giancarli, H. Golfier, A. Hasegawa, Y. Katoh, A. Kohyama, S. Nishio, B. Riccardi, M.S. Tillack, Fus. Eng. Des. 55 (2001) 55.
[2] R.H. Jones, L. Giancarli, A. Hasegawa, Y. Katoh, A. Kohyama, B. Ricarrdi, L.L. Snead, W.J. Weber, J. Nucl. Mater. 307–311 (2002) 1057.
[3] R.J. Price, Nucl. Technol. 35 (1977) 320.
[4] Y. Katoh, H. Kishimoto, A. Kohyama, J. Nucl. Mater. 307–311 (2002) 1221.
[5] CVD Silicon Carbide data sheet, Morton Advanced Materials, Woburn, MA, Rev 1 SiC 9/96.
[6] D.J. Senor, G.E. Youngblood, L.R. Greenwood, D.V. Archer, D.L. Alexander, M.C. Chen, G.A. Newsome, J. Nucl. Mater. 317 (2003) 145.

[7] G.E. Youngblood, D.J. Senor, R.H. Jones, W. Kowbel, J. Nucl. Mater. 307–311 (2002) 1120.
[8] D.J. Senor, G.E. Youngblood, C.E. Moore, D.J. Trimble, G.A. Newsome, J.J. Woods, Fus. Technol. 30 (3) (1996) 943.
[9] M. Rohde, J. Nucl. Mater. 182 (1991) 87.
[10] R.P. Thorne, V.C. Howard, B. Hope, Proceedings of the British Ceramic Society 7 (1967) 449.
[11] G.W. Hollenberg, C.H. Henager, G.E. Youngblood, D.J. Trimble, S.A. Simonson, G.A. Newsome, E. Lewis, J. Nucl. Mater. 219 (1995) 70.